

# Nonlinear left-handed metamaterials

Ilya V. Shadrivov<sup>1</sup>, Alexander A. Zharov<sup>1,2</sup>, Nina A. Zharova<sup>1,3</sup>, and Yuri S. Kivshar<sup>1</sup>

<sup>1</sup>*Nonlinear Physics Centre, Research School of Physical Sciences and Engineering,  
Australian National University, Canberra ACT 0200, Australia*

<sup>2</sup>*Institute for Physics of Microstructures, Russian Academy of Sciences, Nizhny Novgorod 603950, Russia*

<sup>3</sup>*Institute of Applied Physics, Russian Academy of Sciences, Nizhny Novgorod 603600, Russia*

We analyze nonlinear properties of microstructured materials with the negative refractive index, the so-called *left-handed metamaterials*. We demonstrate that the hysteresis-type dependence of the magnetic permeability on the field intensity allows changing the material properties from left- to right-handed and back. Using the finite-difference time-domain simulations, we study the wave reflection from a slab of nonlinear left-handed material, and observe the propagation of *temporal solitons* in such materials. We demonstrate also that nonlinear left-handed metamaterials can support both TE- and TM-polarized self-trapped localized beams, *spatial electromagnetic solitons*. Such solitons appear as single- and multi-hump beams, being either symmetric or antisymmetric, and they can exist due to the hysteresis-type magnetic nonlinearity and the effective domains of negative magnetic permeability.

## I. INTRODUCTION

Recent theoretical studies [1, 2, 3] and experimental results [4, 5, 6] have shown the possibility of creating novel types of microstructured materials that demonstrate many intriguing properties such as the effect of negative refraction. In particular, the composite materials created by arrays of wires and split-ring resonators were shown to possess a negative real part of the magnetic permeability and dielectric permittivity for microwaves. These materials are often referred to as *left-handed materials* (LHMs) or *materials with negative refraction*. Properties of the left-handed materials were analyzed theoretically by Veselago long time ago [7], but such materials were demonstrated experimentally only very recently. As was shown by Veselago [7], the left-handed materials possess a number of peculiar properties, including negative refraction for interface scattering, inverse light pressure, reverse Doppler and Vavilov-Cherenkov effects, etc.

So far, most of the properties of left-handed materials were studied in the linear regime of wave propagation when both magnetic permeability and dielectric permittivity of the material are assumed to be independent on the intensity of the electromagnetic field. However, any future effort in creating *tunable structures* where the field intensity changes the transmission properties of the composite structure would require the study of nonlinear properties of such metamaterials, which may be quite unusual. In particular, the recently fabricated metamaterials are composed of a mesh of wires and split-ring resonators (SRRs). The wires provides negative dielectric permittivity, while SRRs give negative magnetic permeability. Metamaterials possess left-handed properties only in some finite frequency range, which is basically determined by the geometry of the structure. The possibility to control the effective parameters of the metamaterial using nonlinearity has recently been suggested in Refs. [8, 9]. Importantly, the microscopic electric field in the left-handed structure can be much higher than the macroscopic electric field carried by the propagat-

ing wave. This provides a simple physical mechanism for enhancing nonlinear effects in left-handed materials.

In this paper we present a brief overview of nonlinear properties of left-handed metamaterials for the example of a lattice of the split-ring resonators and wires with a nonlinear dielectric. By means of the finite-difference time-domain (FDTD) simulations, we study the wave scattering on a slab of a nonlinear composite structure. We also discuss the structure of electromagnetic solitons supported by the nonlinear left-handed materials with hysteresis-type nonlinear response. We believe our findings may stimulate the future experiments in this field, as well as the studies of nonlinear effects in photonic crystals, where the phenomenon of negative refraction is analyzed now very intensively [10, 11].

## II. NONLINEAR RESONANT RESPONSE

First, we follow the original paper [8] and consider a two-dimensional composite structure consisting of a square lattice of the periodic arrays of conducting wires and split-ring resonators (SRR). We assume that the unit-cell size  $d$  of the structure is much smaller than the wavelength of the propagating electromagnetic field and, for simplicity, we choose the single-ring geometry of a lattice of cylindrical SRRs. The results obtained for this case are qualitatively similar to those obtained in the more involved cases of double SRRs. This type of microstructured materials has recently been suggested and built in order to create left-handed metamaterials with negative refraction in the microwave region [4].

The negative real part of the effective dielectric permittivity of such a composite structure appears due to the metallic wires whereas a negative sign of the magnetic permeability becomes possible due to the SRR lattice. As a result, these materials demonstrate the properties of negative refraction in the finite frequency band,  $\omega_0 < \omega < \min(\omega_p, \omega_{||m})$ , where  $\omega_0$  is the eigenfrequency of the SRRs,  $\omega_{||m}$  is the frequency of the longitudinal

magnetic plasmon,  $\omega_p$  is an effective plasma frequency, and  $\omega$  is the angular frequency of the propagating electromagnetic wave,  $(\mathcal{E}, \mathcal{H}) \sim (\mathbf{E}, \mathbf{H}) \exp(i\omega t)$ . The split-ring resonator can be described as an effective LC oscillator (see, e.g. Ref. [12]) with the capacitance of the SRR gap, as well as an effective inductance and resistance.

Nonlinear response of such a composite structure can be characterized by two different contributions. The first one is an intensity-dependent part of the effective dielectric permittivity of the infilling dielectric. For simplicity, we may assume that the metallic structure is embedded into a nonlinear dielectric with a permittivity that depends on the intensity of the electric field in a general form,  $\epsilon_D = \epsilon_D(|\mathbf{E}|^2)$ . For results of calculations presented below, we take the linear dependence that corresponds to the Kerr-type nonlinear response.

The second contribution into the nonlinear properties of the composite material comes from the lattice of resonators, since the SRR capacitance (and, therefore, the SRR eigenfrequency) depends on the strength of the local electric field in a narrow slot. The intensity of the local electric field in the SRR gap depends on the electromotive force in the resonator loop, which is induced by the magnetic field. Therefore, the effective magnetic permeability  $\mu_{\text{eff}}$  depends on the macroscopic (average) magnetic field  $\mathbf{H}$ , and this dependence can be found in the form [8]

$$\mu_{\text{eff}}(\mathbf{H}) = 1 + \frac{F\omega^2}{\omega_{0NL}^2(\mathbf{H}) - \omega^2 + i\Gamma\omega}, \quad (1)$$

where

$$\omega_{0NL}^2(\mathbf{H}) = \left(\frac{c}{a}\right)^2 \frac{d_g}{[\pi h \epsilon_D(|\mathbf{E}_g(\mathbf{H})|^2)]}$$

is the eigenfrequency of oscillations in the presence of the external field of a finite amplitude,  $h$  is the width of the ring,  $\Gamma = c^2/2\pi\sigma ah$ , for  $h < \delta$ , and  $\Gamma = c^2/2\pi\sigma a\delta$ , for  $h > \delta$ . It is important to note that Eq. (1) has a simple physical interpretation: The resonant frequency of the artificial magnetic structure depends on the amplitude of the external magnetic field and, in turn, this leads to the intensity-dependent function  $\mu_{\text{eff}}$ .

Figures 1 and 2 summarize different types of nonlinear magnetic properties of the composite, which are defined by the dimensionless frequency of the external field  $\Omega = \omega/\omega_0$ , for both a *focusing* [Figs. 1, 2(a,b)] and a *defocusing* [Figs. 1, 2(c,d)] nonlinearity of the dielectric.

Due to the high values of the electric field in the slot of SRR as well as resonant interaction of the electromagnetic field with the SRR lattice, the characteristic magnetic nonlinearity in such structures is much stronger than the corresponding electric nonlinearity. Therefore, *magnetic nonlinearity should dominate* in the composite metamaterials. More importantly, the nonlinear medium can be created by inserting nonlinear elements into the slots of SRRs, allowing an easy tuning by an external field.

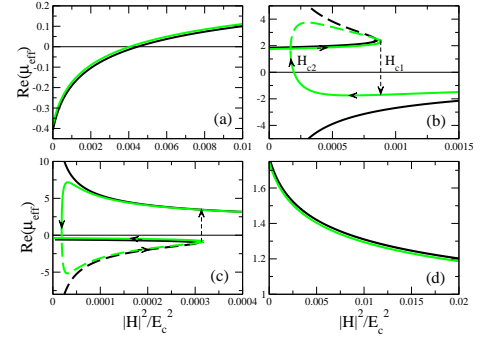


FIG. 1: Real part of the effective magnetic permeability vs. intensity of the magnetic field: (a)  $\Omega > 1$ ,  $\alpha = 1$ ; (b)  $\Omega < 1$ ,  $\alpha = 1$ , (c)  $\Omega > 1$ ,  $\alpha = -1$ ; and (d)  $\Omega < 1$ ,  $\alpha = -1$ . Black – the lossless case ( $\gamma = 0$ ), grey – the lossy case ( $\gamma = 0.05$ ). Dashed curves show unstable branches.

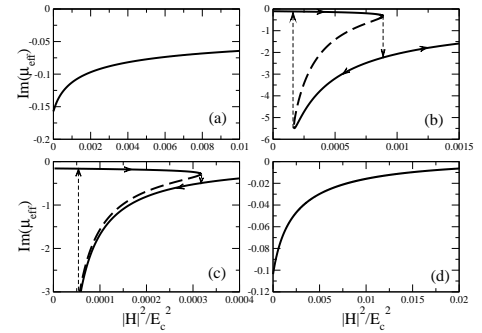


FIG. 2: Imaginary part of the effective magnetic permeability vs. intensity of the magnetic field for  $\gamma = 0.05$ : (a)  $\Omega > 1$ ,  $\alpha = 1$ ; (b)  $\Omega < 1$ ,  $\alpha = 1$ , (c)  $\Omega > 1$ ,  $\alpha = -1$ ; and (d)  $\Omega < 1$ ,  $\alpha = -1$ . Dashed curves show unstable branches.

The critical fields for switching between LH and RH states, shown in the Figs. 1 can be reduced to a desirable value by choosing the frequency close to the resonant frequency of SRRs. Even for a relatively large difference between the SRR eigenfrequency and the external frequency, as we have in Fig. 1(b) where  $\Omega = 0.8$  (i.e.  $\omega = 0.8\omega_0$ ), the switching amplitude of the magnetic field is  $\sim 0.03E_c$ . The characteristic values of the focusing nonlinearity can be estimated for some materials such as n-InSb for which  $E_c = 200V/cm$  [13]. As a result, the strength of the critical magnetic field is found as  $H_{c1} \approx 1.6A/m$ . Strong defocusing properties for microwave frequencies are found in  $Ba_xSr_{1-x}TiO_3$  (see Ref. [14] and references therein). The critical nonlinear field of a thin film of this material is  $E_c = 4 \cdot 10^4 V/cm$ , and the corresponding field of the transition from the LH to RH state [see Fig. 1 (c)] can be found as  $H_c \approx 55.4A/m$ .

The unique possibility of strongly enhanced effective nonlinearities in the left-handed metamaterials revealed here may lead to an essential revision of the concepts based on the linear theory, since the electromagnetic waves propagating in such materials always have a finite amplitude. At the same time, the engineering of non-

linear composite materials may open a number of their novel applications such as frequency multipliers, beam spatial spectrum transformers, switches, limiters, etc.

### III. FDTD SIMULATIONS OF NONLINEAR TRANSMISSION

In order to verify the specific features of the left-handed metamaterials introduced by their nonlinear response, in this section we study the scattering of electromagnetic waves from the nonlinear metamaterial discussed above. In particular, we perform the FDTD numerical simulations of the plane wave interaction with a slab of LHM of a finite thickness. We use the Maxwell's equations in the form

$$\begin{aligned}\nabla \times \mathbf{E} &= -\frac{1}{c} \frac{\partial \mathbf{B}}{\partial t}, \\ \nabla \times \mathbf{B} &= \frac{1}{c} \frac{\partial \mathbf{E}}{\partial t} + \frac{4\pi}{c} \langle \mathbf{j} \rangle + 4\pi \nabla \times \mathbf{M},\end{aligned}\quad (2)$$

where  $\langle \mathbf{j} \rangle$  is the current density averaged over the period of the unit cell, and  $\mathbf{M}$  is the magnetization of the metamaterial. We base our analysis on the microscopic model recently discussed in Ref. [15], and write the constitutive relations in the form

$$\begin{aligned}\sigma L_w S \frac{d \langle \mathbf{j} \rangle}{dt} + \langle \mathbf{j} \rangle &= \frac{\sigma S}{d_{cell}^2} \mathbf{E}, \\ \mathbf{M} &= \frac{n_m}{2c} \pi a^2 I_R \frac{\mathbf{B}}{|\mathbf{B}|},\end{aligned}\quad (3)$$

where  $L_w$  is the inductance of the wire per unit length,  $\sigma$  is the conductivity of metal in the composite,  $S$  is the effective cross-section of a wire,  $S \approx \pi r_w^2$ , for  $\delta > r_w$ , and  $S \approx \pi \delta (2r - \delta)$ , for  $\delta < r_w$ , where  $\delta = c/\sqrt{2\pi\sigma\omega}$  is the skin-layer thickness,  $I_R$  is the current in SRR,  $n_m$  is concentration of SRRs. The current in SRRs is governed by the equation

$$L \frac{dI_R}{dt} = -\frac{\pi a^2}{c} \frac{dH'}{dt} - U - RI_R, \quad (4)$$

where  $L$  is inductance of the SRR,  $R$  is resistance of the SRR wire,  $U$  is the voltage on the SRR slit, and  $H'$  is the acting (microscopic) magnetic field, which differs from the average (macroscopic) magnetic field. Voltage  $U$  at the slit of SRR is coupled to the current  $I$  through the relation

$$C(U) \frac{dU}{dt} = I_R, \quad (5)$$

with

$$C(U) = \pi r^2 \epsilon \left(1 + \alpha |U|^2 / U_c^2\right) / 4\pi d_g,$$

where  $\epsilon$  is the linear part of the permittivity of a dielectric material inside the SRR slit,  $U_c$  is the characteristic nonlinear voltage, and  $\alpha = \pm 1$  corresponds to the case of the focusing and defocusing nonlinear response, respectively.

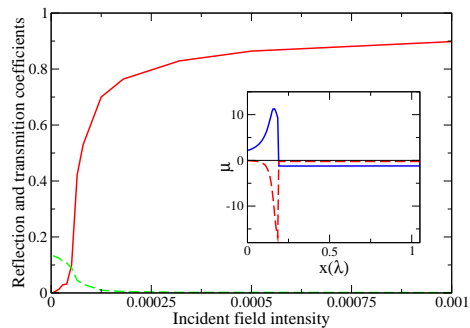


FIG. 3: Reflection (solid) and transmission (dashed) coefficients for a slab of nonlinear metamaterial *vs.* the incident field intensity in a stationary regime, for the case of defocusing nonlinearity ( $\alpha = -1$ ). Inset shows real (solid) and imaginary (dashed) parts of the magnetic permeability inside the slab.

The microscopic magnetic field  $\mathbf{H}'$  can be expressed in terms of  $\mathbf{M}$  and  $\mathbf{B}$  using the Lorenz-Lorentz relation [16]:

$$\mathbf{H}' = \mathbf{B} - \frac{8\pi}{3} \mathbf{M}. \quad (6)$$

As a result, Eqs. (2) to (6) form a closed system of coupled equations, and they can be solved numerically using, for example, the numerical FDTD method. We also notice that, by substituting the harmonic fields into these equations, we recover the expression for the magnetic permeability (1).

Our goal is to study the temporal dynamics of the wave scattering by a finite slab of nonlinear metamaterial. For simplicity, we consider a one-dimensional problem that describes the interaction of the plane wave incident at the normal angle from air on a slab of metamaterial of a finite thickness. We consider *two types of nonlinear effects*: (i) nonlinearity-induced suppression of the wave transmission when initially transparent left-handed material becomes opaque with the growth of the input amplitude, and (ii) nonlinearity-induced transparency when an opaque metamaterial becomes left-handed (and therefore transparent) with the growth of the input amplitude. The first case corresponds to the dependence of the effective magnetic permeability on the external field shown in Figs. 1(a,c), when initially negative magnetic permeability (we consider  $\epsilon < 0$  in all frequency range) becomes positive with the growth of the magnetic field intensity. The second case corresponds to the dependence of the magnetic permeability on the external field shown in Figs. 1(b).

In all numerical simulations, we use *linearly growing* amplitude of the incident field within the first 50 periods, that becomes constant afterwards. The slab thickness is selected as  $1.3\lambda_0$  where  $\lambda_0$  is a free-space wavelength. For the parameters we have chosen, the metamaterial is left-handed in the linear regime for the frequency range from  $f_1 = 5.787$  GHz to  $f_2 = 6.05$  GHz.

Our simulations show that for the incident wave with

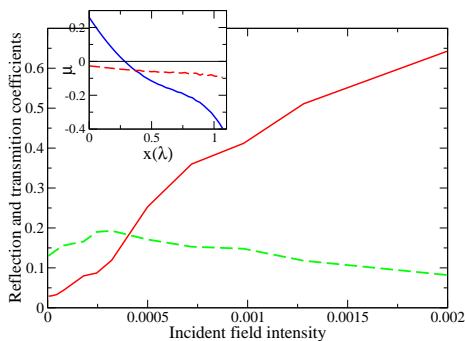


FIG. 4: Reflection (solid) and transmission (dashed) coefficients for a slab of nonlinear metamaterial *vs.* the incident field intensity in a stationary regime, for the focusing nonlinearity ( $\alpha = 1$ ). Inset shows real (solid) and imaginary (dashed) parts of the magnetic permeability inside the slab.

the frequency  $f_0 = 5.9$  GHz (i.e. inside the left-handed transmission band), electromagnetic field reaches a steady state independently of the sign of the nonlinearity. Both reflection and transmission coefficients in the *stationary* regime are shown in Figs. 3,4 as functions of the incident field amplitude, for both defocusing and focussing nonlinear response of the dielectric infilling the SRR slits. In the linear regime, the effective parameters of the metamaterial at the frequency  $f_0$  are:  $\epsilon = -1.33 - 0.01i$  and  $\mu = -1.27 - 0.3i$ ; this allows excellent impedance matching with surrounding air. The scattering results in a vanishing reflection coefficient for small incident intensities (see Figs. 3,4).

Reflection and transmission coefficients are qualitatively different for two different types of infilling nonlinear dielectric. For the defocusing nonlinearity, the reflection coefficient varies from low to high values when the incident field exceeds some threshold value (see Fig. 3). Such a sharp transition can be explained in terms of the hysteresis behavior of the magnetic permeability shown in Fig. 1(c). When the field amplitude in metamaterial becomes higher than the critical amplitude [shown by a dashed arrow in Fig. 1(c)], magnetic permeability changes its sign, and the metamaterial becomes opaque. Our FDTD simulations show that for overcritical amplitudes of the incident field, the opaque region of positive magnetic permeability appears inside the slab (see the inset in Fig. 3). The magnetic permeability experiences an abrupt change at the boundary between the transparent and opaque regions. The dependencies shown in Fig. 3 are obtained for the case when the incident field grows from zero to a steady-state value. However, taking different temporal behavior of the incident wave, e.g. increasing the amplitude above the threshold value and then decreasing it to the steady state, one can get different values of the stationary reflection and transmission coefficients, and different distributions of the magnetic permeability inside the metamaterial slab. Such properties of the nonlinear metamaterial slab are consistent with the predicted multi-valued dependence of the mag-

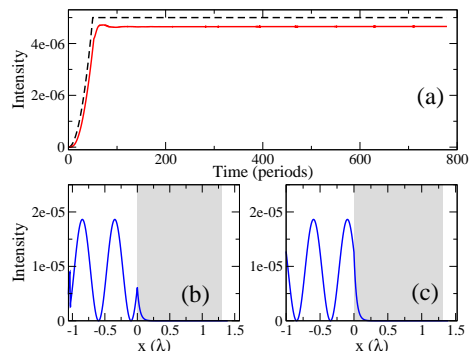


FIG. 5: (a) Reflected (solid) and incident (dashed) wave intensity *vs.* time for small amplitudes of the incident wave (i.e. in the linear regime). (b,c) Distribution of the magnetic and electric fields at the end of simulation time; the metamaterial is shaded.

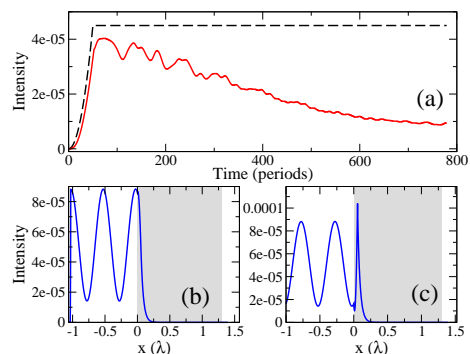


FIG. 6: The same as in Fig. 5 but in the regime of overcritical amplitude of the incident wave.

netic permeability on the amplitude of the magnetic field.

In the case of focussing nonlinearity (see Fig. 4), the dependence of the reflection and transmission coefficients on the amplitude of the incident field is smooth. This effect originates, firstly, from a gradual detuning from the impedance matching condition, and, for higher powers, from the appearance of an opaque layer (see the inset in Fig. 4) with a positive value of the magnetic permeability that is a continuous function of the coordinate inside the slab.

Now we consider another interesting case when initially opaque metamaterial becomes transparent with the growth of the incident field amplitude. We take the frequency of the incident field to be  $f_0 = 5.67$  GHz, so that magnetic permeability is positive in the linear regime and the metamaterial is opaque. In the case of self-focussing nonlinear response ( $\alpha = 1$ ), it is possible to switch the material properties to the regime with negative magnetic permeability [see Fig.1(b) making the material slab left-handed and therefore transparent. Moreover, one can expect the formation of self-focused localized states inside the composite, the effect which was previously discussed for the interaction of the intense electromagnetic waves with over-dense plasma [17]. Figure 5(a) shows the

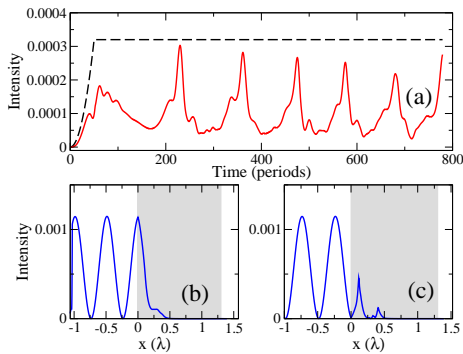


FIG. 7: The same as in Fig. 5 but in the regime of strongly overcritical amplitude of the incident wave.

temporal evolution of the incident and reflected wave intensities for small input intensities, this case corresponds to the linear regime. The reflection coefficient reaches a steady state after approximately 100 periods. The spatial distribution of the electric and magnetic fields at the end of simulation time is shown in Fig. 5(b,c), respectively.

In a weakly nonlinear overcritical regime (see Fig. 6), the intensity of the reflected beam decreases approaching a steady state. In this case we observe the formation of a localized state inside the metamaterial slab and near the interface, as can be seen more distinctly in Fig. 6(c). This effect give an additional contribution to the absorption of the electromagnetic energy, thus leading to a decay of the value of the reflection coefficient.

In a strongly nonlinear overcritical regime, we observe the effect of the dynamical self-modulation of the reflected electromagnetic wave that results from the periodic generation of the self-localized states inside the metamaterial (see Fig. 7). Such localized states resemble *temporal solitons*, which transfer the energy away from the interface. Figure 7(c) shows an example when two localized states enter the metamaterial. These localized states appear on the jumps of the magnetic permeability and, as a result, we observe a change of the sign of the electric field derivative at the maximum of the soliton intensity, and subsequent appearance of transparent regions in the metamaterial. Unlike all previous cases, the field structure in this regime do not reach any steady state for high enough intensities of the incident field.

#### IV. ELECTROMAGNETIC SPATIAL SOLITONS

Similar to other nonlinear media [19], nonlinear left-handed composite materials can support self-trapped electromagnetic waves in the form of *spatial solitons*. Such solitons possess interesting properties because they exist in materials with a hysteresis-type (multi-stable) nonlinear magnetic response. Below, we describe novel and unique types of single- and multi-hump (symmetric, antisymmetric, or even asymmetric) backward-wave spatial electromagnetic solitons supported by the nonlinear

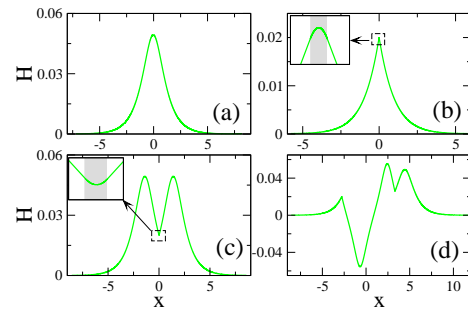


FIG. 8: Examples of different types of solitons: (a) fundamental soliton; (b,c) solitons with one domain of negative or positive magnetic permeability (shaded), respectively; (d) soliton with two different domains (shaded). Insets in (b,c) show the magnified regions of the steep change of the magnetic field.

magnetic permeability.

Spatially localized TM-polarized waves that are described by one component of the magnetic field and two components of the electric field. Monochromatic stationary waves with the magnetic field component  $H = H_y$  propagating along the  $z$ -axis and homogeneous in the  $y$ -direction,  $[\sim \exp(i\omega t - ikz)]$ , are described by the dimensionless nonlinear Helmholtz equation

$$\frac{d^2 H}{dx^2} + [\epsilon\mu(|H|^2) - \gamma^2]H = 0, \quad (7)$$

where  $\gamma = kc/\omega$  is a wavenumber,  $x = x'\omega/c$  is the dimensionless coordinate, and  $x'$  is the dimensional coordinate. Different types of localized solutions of Eq. (7) can be analyzed on the phase plane  $(H, dH/dx)$  (see, e.g., Refs. [18]). First, we find the equilibrium points: the point  $(0, 0)$  existing for all parameters, and the point  $(0, H_1)$ , where  $H_1$  is found as a solution of the equation

$$X^2(H_1) = X_{\text{eq}}^2 = \Omega^2 \left\{ 1 + \frac{F\epsilon_{\text{eff}}}{(\gamma^2 - \epsilon_{\text{eff}})} \right\}. \quad (8)$$

Below the threshold, i.e. for  $\gamma < \gamma_{\text{tr}}$ , where  $\gamma_{\text{tr}}^2 = \epsilon[1 + F\Omega^2/(1 - \Omega^2)]$ , the only equilibrium state  $(0, 0)$  is a saddle point and, therefore, no finite-amplitude or localized waves can exist. Above the threshold value, i.e. for  $\gamma > \gamma_{\text{tr}}$ , the phase plane has three equilibrium points, and a separatrix curve corresponds to a soliton solution.

In the vicinity of the equilibrium state  $(0, 0)$ , linear solutions of Eq. (7) describe either exponentially growing or exponentially decaying modes. The equilibrium state  $(0, H_1)$  describes a finite-amplitude wave mode of the transverse electromagnetic field. In the region of multi-stability, the type of the phase trajectories is defined by the corresponding branch of the multi-valued magnetic permeability. Correspondingly, different types of the spatial solitons appear when the phase trajectories correspond to the different branches of the nonlinear magnetic permeability.

The fundamental soliton is described by the separatrix trajectory on the plane  $(H, dH/dx)$  that starts at the point  $(0, 0)$ , goes around the center point  $(0, H_1)$ , and then returns back; the corresponding soliton profile is shown in Fig. 8(a). More complex solitons are formed when the magnetic permeability becomes multi-valued and is described by several branches. Then, soliton solutions are obtained by switching between the separatrix trajectories corresponding to different (upper and lower) branches of magnetic permeability. Continuity of the tangential components of the electric and magnetic fields at the boundaries of the domains with different values of magnetic permeability implies that both  $H$  and  $dH/dx$  should be continuous. As a result, the transitions between different phase trajectories should be continuous.

Figures 8(b,c) show several examples of the more complex solitons corresponding to a single jump to the lower branch of  $\mu(H)$  (dotted) and to the upper branch of  $\mu(H)$  (dashed), respectively. The insets show the magnified domains of a steep change of the magnetic field. Both the magnetic field and its derivative, proportional to the tangential component of the electric field, are continuous. The shaded areas show the effective domains where the value of magnetic permeability changes. Figure 8(d) shows an example of more complicated multi-hump soliton which includes two domains of the effective magnetic permeability, one described by the lower branch, and the other one – by the upper branch. In a similar way, we can find more complicated solitons with different number of domains of the effective magnetic permeability.

We note that some of the phase trajectories have discontinuity of the derivative at  $H = 0$  caused by infinite values of the magnetic permeability at the corresponding branch of  $\mu_{\text{eff}}(H)$ . Such a non-physical effect is an artifact of the lossless model of a left-handed nonlinear composite considered here for the analysis of the soliton solutions. In more realistic models that include losses, the region of multi-stability does not extend to the point  $H = 0$ , and in this limit the magnetic permeability remains a single-valued function of the magnetic field [8].

For such a multi-valued nonlinear magnetic response, the domains with different values of the magnetic permeability "excited" by the spatial soliton can be viewed

as effective induced left-handed waveguides which make possible the existence of single- and multi-hump soliton structures. Due to the existence of such domains, the solitons can be not only symmetric, but also antisymmetric and even asymmetric. Formally, the size of an effective domain can be much smaller than the wavelength and, therefore, there exists an applicability limit for the obtained results to describe nonlinear waves in realistic composite structures.

When the infilling dielectric of the structure displays *self-focusing nonlinear response*, we have  $\Omega < 1$ , and in such system we can find *dark solitons*, i.e. localized dips on the finite-amplitude background wave [19]. Similar to bright solitons, there exist both fundamental dark solitons and dark solitons with domains of different values of magnetic permeability. For self-defocusing nonlinearity and  $\Omega < 1$ , magnetic permeability is a single-valued function, and such a nonlinear response can support dark solitons as well, whereas for self-focusing dielectric, we have  $\Omega > 1$  and no dark solitons can exist.

## V. CONCLUSIONS

We have discussed novel properties of left-handed metamaterials associated with their nonlinear resonant response. For the case of harmonic fields, we have calculated the effective magnetic permeability of microstructured materials consisting of rods and split-ring resonators, and predicted the hysteresis-like dependence of the nonlinear magnetic permeability as a function of the applied magnetic field. Using the finite-difference time-domain numerical simulations, we have studied the temporal dynamics of the wave reflection from a slab of nonlinear metamaterial that is found to be consistent with our theory. Finally, we have predicted the existence of electromagnetic spatial solitons supported by the hysteresis-type nonlinear magnetic permeability of a left-handed material.

The work has been supported by the Australian Research Council and the Australian National University.

- 
- [1] J.B. Pendry, A.J. Holden, W.J. Stewart, and I. Youngs, Phys. Rev. Lett. **76**, 4773 (1996).
  - [2] J.B. Pendry, A.J. Holden, D.J. Robbins, W.J. Stewart, IEEE Trans. Microwave Theory Tech. **47**, 2075 (1999).
  - [3] P. Markos and C.M. Soukoulis, Phys. Rev. E **65**, 036622(2002); Phys. Rev. B **65**, 033401 (2002).
  - [4] D.R. Smith, W. Padilla, D.C. Vier, S.C. Nemat-Nasser, and S. Shultz, Phys. Rev. Lett. **84**, 4184 (2000).
  - [5] M. Bayindir, K. Aydin, E. Ozbay, P. Markos, and C. M. Soukoulis, Appl. Phys. Lett. **81**, 120 (2002).
  - [6] C.G. Parazzoli, R.B. Greigor, K. Li, B.E.C. Koltenbah, and M. Tanielian, Phys. Rev. Lett. **90**, 107401 (2003).
  - [7] V. G. Veselago, Usp. Fiz. Nauk, **92**, 517 (1967) (in Russian) [Sov. Phys. Uspekhi **10**, 509 (1968)].
  - [8] A.A. Zharov, I.V. Shadrivov, and Yu.S. Kivshar, Phys. Rev. Lett. **91**, 037401 (2003).
  - [9] M. Lapine, M. Gorkunov, and K.H. Ringhofer, Phys. Rev. E **67**, 065601 (2003).
  - [10] C. Luo, S.G. Johnson, and J. D. Joannopoulos, Appl. Phys. Lett. **83**, 2352 (2002).
  - [11] C. Luo, S.G. Johnson, J.D. Joannopoulos, J.B. Pendry, Phys. Rev. B **65**, 201104(R) (2002).
  - [12] M. Gorkunov, M. Lapine, E. Shamonina, and K.H. Ringhofer, Eur. Phys. J. **B 28**, 263 (2002).

- [13] A. M. Belyantsev, V. A. Kozlov and V. I. Piskaryov, *Infrared Physics* **21**, 79 (1981).
- [14] H. Li, A. L. Roytburd, S. P. Alpay, T. D. Tran, L. Salamanca-Riba, and R. Ramesh, *Appl. Phys. Lett.* **78**, 2354 (2001).
- [15] I.V. Shadrivov, N.A. Zharova, A.A. Zharov, and Yu.S. Kivshar, *Phys. Rev. E* **70** (2004) (in press).
- [16] M. Born and E. Wolf, *Principles of Optics: Electromagnetic Theory of Propagation, Interference and Diffraction of Light* (Cambridge University Press, UK, 2002).
- [17] K. Zauer, L. M. Gorbunov, *Fizika Plazmy*, **3**, 1302 (1977) (in Russian); A. A. Zharov, A. K. Kotov, *Fizika Plazmy*, **10**, 615 (1984) (in Russian) [*Sov. J. Plasma Phys.* **10**, 359 (1984)]; A. V. Kochetov, A. M. Feigin, *Fizika Plazmy*, **14**, 716 (1988) (in Russian) [*Sov. J. Plasma Phys.*, **14**, 423 (1988)].
- [18] V. B. Gil'denburg, A. V. Kochetov, A. G. Litvak, and A. M. Feigin, *Sov. Phys. JETP* **57**, 28 (1983)(in Russian)[*Zh. Eksp. Teor. Fiz.* **84**, 48 (1983)].
- [19] For a comprehensive overview of spatial solitons in nonlinear optics, see Yu.S. Kivshar and G.P. Agrawal, *Optical Solitons: From Fibers to Photonic Crystals* (Academic Press, San Diego, 2003), 540 pp.